Letter

Electronic origin of x-ray absorption peak shifts

S. Shallcross,[1] C. v. Korff Schmising,[1] P. Elliott,[1] S. Eisebitt,[1] J. K. Dewhurst,[2] and S. Sharma[1,*]
[1]*Max Born Institute for Nonlinear Optics and Short Pulse Spectroscopy, Max-Born-Straße 2A, 12489 Berlin, Germany*
[2]*Max-Planck-Institut fur Mikrostrukturphysik Weinberg 2, 06120 Halle, Germany*

(Received 22 May 2022; revised 14 July 2022; accepted 3 August 2022; published 15 August 2022)

Encoded in the transient x-ray absorption (XAS) and magnetic circular (MCD) response functions resides a wealth of information of the microscopic processes of ultrafast demagnetization. Employing state-of-the-art first-principles dynamical simulations we show that the experimentally observed energy shift of the L_3 XAS peak in Ni, and the absence of a corresponding shift in the dichroic MCD response, can be explained in terms of laser-induced changes in band occupation. Strikingly, we predict that for the same ultrashort pump pulse applied to Co the opposite effect will occur: a substantial shift upward in energy of the MCD peaks will be accompanied by very small change in the position of XAS peaks, a fact we relate to the reduced d-band filling of Co that allows a greater energetic range above the Fermi energy into which charge can be excited. We also carefully elucidate the dependence of this effect on pump pulse parameters. These findings (i) establish an electronic origin for early-time peak shifts in transient XAS and MCD spectroscopy and (ii) illustrate the rich information that may be extracted from transient response functions of the underlying dynamical system.

DOI: 10.1103/PhysRevB.106.L060302

The ultrafast control over magnetic solids by light has opened new vistas in fundamental condensed matter physics [1–6] that, with the recent introduction of first-principles simulations [7–9] capable of very accurately treating the early-time regime (less than a few hundred femtoseconds), can now be explored in tandem by theoreticians and experimentalists [10,11]. Experimentally, the measurement of dynamically evolving magnets on femtosecond to picosecond timescales rests upon spectroscopic probes, with two of the key methods transient x-ray absorption spectroscopy (XAS) and transient magnetic circular dichroism (MCD) [12–20]. In these techniques a laser-pumped magnetic material is perturbed with helicity-dependent (i.e., left and right circularly polarized) light, the frequency of which resonates with the core level of one of the constituent atoms, and the response then recorded as a function of time. The normalized difference of these two helicity-dependent response functions is proportional to the MCD, and represents the magnetic response of the material, while their sum is proportional to the XAS, and represents the charge response of the material.

Integrating the MCD and XAS spectra via the sum rules [14,15,21] yields species-resolved magnetic moments, a procedure that is rigorous for atoms and, while less rigorous, represents a "tried and tested" method for probing magnetism in solids, both in the ground state as well as in laser-induced dynamical states. It is clear, however, that a wealth of information of the underlying dynamical processes is encoded in transient response functions [18,20,22–24], with the extraction of magnetic moments representing only one possibility. A crucial task at the frontier of ultrafast spectroscopy is therefore interpreting the temporal evolution of spectral structures such as peak centers and widths: what insight into the underlying microscopic physics of ultrafast demagnetization can be extracted from such spectral changes?

In laser-pumped Ni it was observed that in addition to the reduction in amplitude of the MCD and XAS peaks, well-known signatures of laser-induced demagnetization, the XAS peak shifts noticeably to lower energies [12] with, in contrast, the MCD peak exhibiting no such shift [18,22,25]. While the reduction in peak amplitudes can be understood in terms of the excitation of charge and a concomitant high rate of spin-orbit-induced transitions from majority to minority, physics captured by the sum rules, the XAS peak shift, and the absence of such a shift in the MCD spectrum, has defied microscopic analysis. Connecting features of spin and charge response functions to underlying microscopic processes is in general a difficult task, and is made more so in the highly nonequilibrium situation of laser-induced demagnetization by the several distinct demagnetization processes that occur. This is reflected in the rather disparate set of explanations that have been put forward for the XAS peak shift in Ni: thermal effects [25], magnon excitation [22], and band mirroring [18] have all been considered. Theoretically, response functions derived from the static picture with redistribution of charge were found not to be able to explain this difference between the behavior of the XAS and MCD peaks [26].

In the present work, by performing fully quantum-mechanical state-of-the-art dynamical calculations [27–29], we resolve this existing controversy concerning the

*sharma@mbi-berlin.de

interpretation of XAS and MCD spectral shifts in Ni. We find, in agreement with experiment, a shift downward in photoenergy of the XAS peak with almost no corresponding shift upward of the MCD peak; moreover we predict that in Co pumped with an ultrashort laser pulse, remarkably, this effect is inverted: a large shift of the MCD peaks toward higher photon energies is accompanied by a very small shift of the XAS peak. The origin of both these effects we locate in specific features of the electronic spectrum near the chemical potential, with the increased d-band filling of Ni as compared to Co playing an important role. The XAS and MCD peak shifts in Ni and Co are thus shown to be a purely electronic effect resulting from laser-induced changes in band occupation, providing an example of how XAS and MCD response functions may yield insight into the underlying spin dynamics beyond that provided by their use in the determination of dynamical spin moments.

Computational details. To calculate the spin dynamics of laser-pumped Ni and Co we have used the fully *ab initio* state-of-the-art, fully noncollinear spin-dependent version [30,31] of time-dependent density functional theory (TDDFT) [32]. Note that the presence of spin-orbit coupling breaks the SU(2) spin symmetry and mixes both spin channels, in turn requiring the fully noncollinear treatment of spin that we employ. In the present work we have used the adiabatic local density approximation for the exchange-correlation potential and all calculations are performed using the highly accurate full potential linearized augmented-plane-wave method [33], as implemented in the ELK [31,34] code. A face-centered-cubic unit cell with lattice parameter of 3.21 Å was used for Co, while for Ni a lattice parameter of 3.53 Å was used. The Brillouin zone was sampled with a $20 \times 20 \times 20$ k-point mesh for both materials. For time propagation the algorithm detailed in Ref. [31] was used with a time step of 2.42 attoseconds. The final magnetization value converges with the above-mentioned computational parameters to $1.67\mu_B$ for Co and $0.61\mu_B$ for Ni.

In order to calculate transient XAS and MCD spectra for laser-pumped Ni and Co at various times, the linear response formalism of the TDDFT is the used [32,35,36]. This method [27] is equivalent to probing the system without accounting for the width of the probe pulse. Despite this we found that the transient response functions are in excellent agreement with experiments [23,27]. In calculating the response functions we use 23 **G** vectors to capture local field effects, the bootstrap kernel to treat excitonic effects, and a smearing of 0.9 eV that is derived from the *GW*-calculated average width of the semicore $p_{3/2}$ and $p_{1/2}$ L peaks. The positions of the $2p$ states were also determined via the *GW* method, with the scissors-corrected KS states used in calculating the response functions. The *GW* calculations were performed at a temperature of 500 K using the spin-polarized *GW* method [37]. The spectral function on the real axis is constructed using a Padé approximation with spin-orbit coupling included and a Matsubara cutoff of 12 Ha used. We find that the static XAS and MCD spectra calculated with these parameters reproduce previous theoretical simulations [38,39] and are in good agreement with experiments [21,25].

Transient XAS and MCD. It is well established in experiment that pumping with laser light leads to demagnetization of both Ni and Co. This change in the moment can be determined by integrating the MCD and XAS spectra and using the sum rules [14,15,21]. However, this requires fully energy- and time-resolved spectra, which is experimentally very difficult to determine. The signature of this loss in spin moment also can be determined by just looking at the reduction in the peak (L_3 and L_2) height in XAS and MCD spectra. For Ni this reduction can be experimentally observed in the MCD spectra. Together with this reduction, the XAS (L_3 edge) shows a substantial shift to lower energy, while the MCD spectra do not shift and several scenarios have been proposed to explain this [18,22,25].

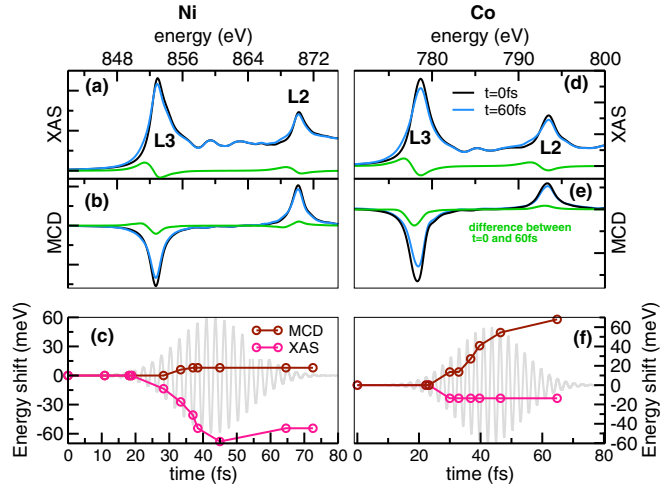

FIG. 1. XAS, MCD, and L edge peak shifts for Ni and Co. Shown in panels (a) and (b) respectively are the XAS and MCD spectra before and after ($t = 60$ fs) laser pumping for Ni, with the difference shown in green. The energy shift of the XAS and MCD L_3 peak (on meV) as a function of time is shown in panel (c), revealing a substantial shift down in energy of the XAS peak but almost no shift in the MCD L_3 peak. Panels (d)–(f): Corresponding data for Co. In dramatic contrast to Ni, for this material it is the MCD that shows a substantial shift (upward) in energy. In both cases the same 1.55 eV linearly polarized pump pulse (with polarization parallel to the spin-quantization axis) was used with fluence 6.7 mJ/cm^2, full width at half maximum 24.5 fs, and intensity 7.2×10^{12} W/cm^2; the **A** field of this pump pulse is shown in gray in panels (c) and (f).

To examine this, in Figs. 1(a) and 1(b) we show the calculated XAS and MCD response function before ($t = 0$) and after ($t = 60$ fs) laser pumping along with their difference. A linearly polarized pump pulse (with polarization vector parallel to the spin-quantization axis) of fluence 6.7 mJ/cm^2, duration 24.5 fs, and a central frequency of 1.55 eV is used. From examination of the XAS it can be discerned that the L_3 peak at 60 fs has shifted to lower energies. Furthermore, the weight of the XAS is also shifted to lower energies. The MCD spectra at the L_3 edge merely broaden and reduce in amplitude. The difference of the XAS signal between $t = 0$ and $t = 60$ fs exhibits a signature bipolar behavior: a decrease in XAS at L_3 and L_2 edges is accompanied by an increase at energies below L_3 and L_2 edges. This is expected as the total charge is conserved, so that a decrease at the resonance must be accompanied by an increase at lower energies. Often this bipolar behavior is inferred as an indication of the shifting

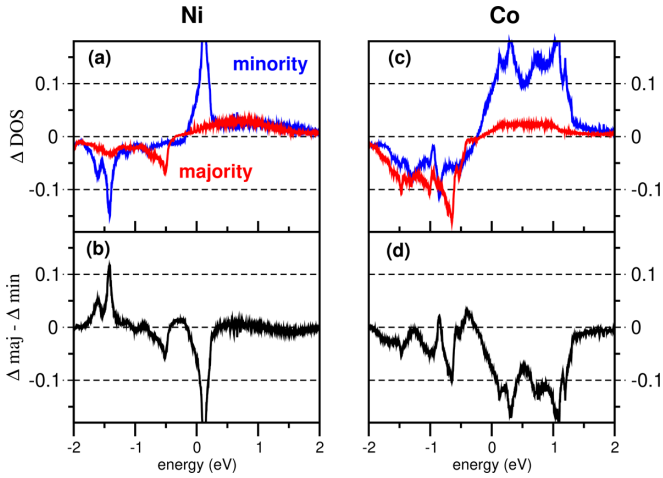

FIG. 2. Difference in the spin and d-state projected DOS (in states/eV/spin) before and 60 fs after pumping for (a) Ni and (c) Co. The energy-resolved change in moment (in μ_B) from the ground state to 60 fs after pumping for (b) Ni and (d) Co. The pump pulse is linearly polarized with polarization direction parallel to the spin-quantization axis. In both cases the same 1.55 eV pump pulse was used with fluence 6.7 mJ/cm^2, full width at half maximum 24.5 fs, and intensity 7.2×10^{12} W/cm^2.

of the peak to lower energy; however this is generally not correct, and such bipolar behavior indicates only a shifting of the spectral weight to lower energy which might not be accompanied by a shift of the peak center. To unveil the dynamics of the XAS and MCD peak shifts in Fig. 1(c) we plot the peak centers as a function of time. Exactly as experiments report we see a substantial shift of the XAS L_3 edge peak, that begins at the start of the pulse and is largely complete at the maximum of the pump pulse envelope. Again as seen in experiment the MCD peak does not show a significant shift in position with a maximum shift of +8 meV to higher energies, approximately an order of magnitude smaller than the XAS peak shift downward in energy.

Since the L edge XAS is a direct probe of the available d states and MCD of the spin-projected available d states for transition from the exchange-split $2p$ states [28,29], we now take a closer look at the transient occupied density of states (DOS) [40]. In Fig. 2(a) we present the difference in the transient occupied d-band DOS for Ni after the pump pulse (60 fs) and occupied d-band DOS of the ground state. Note therefore that in this figure positive ΔDOS indicates the laser-induced occupation of states, and negative ΔDOS the creation of empty d states. A striking feature can immediately be observed in the narrow energy range of minority channel excited charge just above E_F. This ∼0.5 eV region of laser-excited charge contrasts with the situation below E_F in which empty states of minority and majority charge have been created over a wide energy range of ∼2 eV. These empty states are created both due to laser excitation as well as due to spin-orbit-mediated spin flips. The origin of the peak shift to lower energies is now clearly revealed: as the XAS response function measures transitions from the $2p$ states to unoccupied valence states, above E_F the response function will be reduced in a narrow energy window, while below E_F the response will be increased in a wide energy range. Taken together, this can only result in a shift to lower energies of the L_3 (as well as L_2) peak centers and spectral weight.

For elucidating the nonshifting of the MCD peak the relevant quantity is the difference of the two ΔDOS (majority and minority), i.e., the energy-resolved change in moment from the ground state. This change in moment is shown in Fig. 2(b) for $t = 60$ fs (after the pump pulse), revealing that this quantity shows two almost symmetrically (in energy) placed peaks around E_F (0.2 eV above and 0.5 eV below E_F); however, the peak above E_F is much larger in magnitude (note the opposite sign of the peak simply follows from the fact that we plot in ΔDOS the difference of majority and minority DOS, and the system has suffered an overall loss of moment). Following the same argumentation of the XAS response function, this would be expected to lead to a shift in the MCD peak to higher energies and a broadening of the peak with spectral weight shifting also to lower energies (due to a peak 0.5 eV below E_F). However, as the peak above E_F resides in very narrow energy window the shift will be small. This is exactly what is seen in Fig. 1(c). In experiment this small shift is probably not resolvable and thus these results are consistent with the reported nonshifting of the MCD peak.

It is clear that the laser-induced changes of occupation revealed in Fig. 2 represent a complex dynamical change in band occupation that is highly asymmetric about E_F, occurs over a wide range of energies, and is material specific. A simplistic model in which the occupation function is symmetrically manipulated will hence not be expected to capture the underlying physics of peak shifts [26], which requires a fully dynamical quantum-mechanical description for their explanation.

Having established that the L_3 edge peak shift in Ni has an electronic origin, it is of interest to examine the corresponding spectral feature in neighboring Co. In Figs. 2(c) and 2(d) we show the change in DOS for both spin channels and the energy-resolved change in moment for Co. We employ the same pulse parameters as used for Ni and again show the change in d-DOS and energy-resolved moment between 60 fs (after the pulse) and the ground state.

Comparison with Ni reveals a strikingly different behavior occurs in laser-pumped Co. Whereas Ni exhibited a minority peak restricted to a narrow 0.5 eV range above E_F, for Co minority excitations occur over a broad range in energy: both minority and majority are excited from a 2 eV range below E_F into the minority states in a similarly broad energy range of up to 2 eV above E_F. The L edge response is thus not expected to exhibit as pronounced a shift in its central peak as in the case of Ni. Turning to the XAS spectra for Co in Fig. 1(d) and the corresponding peak shift plotted in Fig. 1(f) we see this is exactly what occurs: the L_3 peak center shifts by a very small value of 20 meV.

In contrast to the charge excitation the energy-resolved change in moment from the ground state shows a significant skew about E_F [see Fig. 2(d)]. This should then result in a pronounced decrease of the leading edge of the L_3 of the MCD peak, resulting in a shift of these MCD spectra to higher energies. Again, inspection of the MCD spectra of Co in Fig. 1(e) and the corresponding peak shift plotted in Fig. 1(f) reveals exactly the behavior expected on the basis

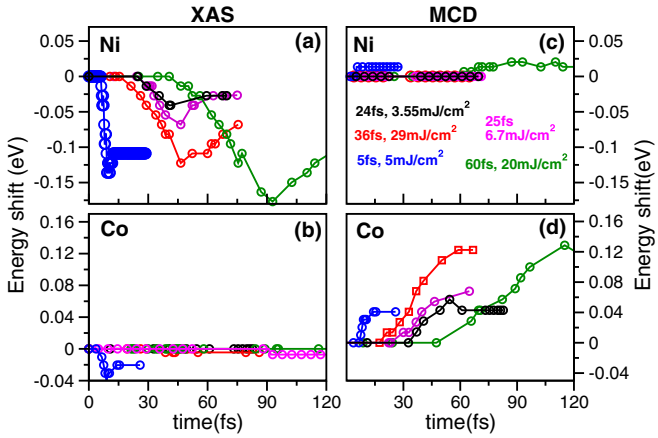

FIG. 3. Dynamics of L_3 peak position upon laser pumping: XAS L_3 peak for (a) Ni and (b) Co. MCD L_3 peak for (c) Ni and (d) Co. The linearly polarized pump laser pulses (with polarization parallel to the spin-quantization axis) have a central frequency of 1.55 eV, with the duration and incident fluence as shown in the legend. The Ni XAS and Co MCD L_3 peaks show a shift independent of the pulse parameters; however the amount of the shift depends strongly upon the pump pulse. In contrast, the Ni MCD and Co XAS peaks display almost no shift, a fact that holds for all pulse parameters.

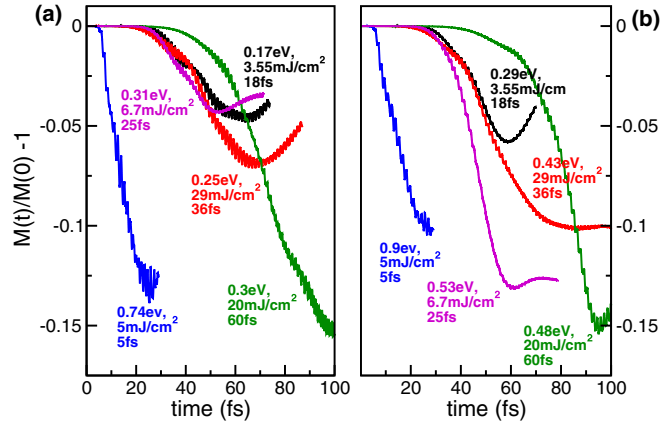

FIG. 4. Normalized change in moment as a function of time in laser pumped (a) Ni and (b) Co. The central frequency of all the pulses is 1.55 eV. The duration (in fs), the incident fluence (in mJ/cm^2), and the absorbed energy per unit volume (in eV) are quoted in the legend. For all cases these pump pulses are linearly polarized with polarization parallel to the spin-quantization axis. As in experiments, we find that for a given absorbed energy, Ni demagnetizes more that Co.

of this underlying electronic rearrangement of the moment: a dramatic shift upward in energy of the MCD peak by 60 meV.

Dependence of the peak shifts on laser pulse parameters. Thus far we have probed the shifting of spectral peaks in the XAS and MCD via a single set of laser pulse parameters, and we thus now examine the impact of the form of the laser pulse on the shifting of the XAS and MCD L edge peaks. In Fig. 3 is shown the XAS and MCD peak shift in Ni and Co, for a wide range of pulse parameters. As can be seen for Ni in each case the XAS L_3 peak shifts downward in energy [see Fig. 3(a)], by up to 150 meV, while the MCD L_3 peak [see Fig. 3(c)] shows almost no shift (maximum being 20 meV). In Co the MCD L_3 peak [see Fig. 3(d)] shifts always upward in energy, by up to 120 meV, while the XAS L_3 peak [see Fig. 3(c)] shows very small downward shift, with a maximum value of 40 meV. The amount of the shift is dependent upon the laser pulse parameters. The magnitude of the XAS peak shift in Ni corresponds very closely to the size of the laser-induced demagnetization, as may be seen by comparison of the peak shift [Fig. 3(a)] and normalized moment loss [Fig. 4(a)]. In the case of the MCD shift in Co such a clear link is not seen, with the loss of moment quite different for laser pulses that lead to similar peak shift. This corresponds with the more complex underlying electronic behavior: the dramatic skew about E_F in moment loss is a result of both (i) optical (spin preserving) transitions from minority below to above E_F as well as (ii) spin-orbit-induced transitions from majority into minority below E_F. The skew of moment loss about E_F will evidently depend on how these two processes compensate each other, which is expected to be rather sensitive to pulse parameters.

It is important to note that for a given absorbed fluence Ni demagnetizes more than Co. However, we find that for fixed pulse parameters Co absorbs more than Ni. This is due to nonlinear effects that result in excitations far above the Fermi level, up to 6 eV above the Fermi level as shown in a recent experimental investigation [41]. Such states, however, have very short lifetime and thus quickly decay to lower energy states by scattering events, resulting in additional transitions to lower energy states. This decay of high-energy states is not included in our theoretical approach. We can, however, determine the energy "locked in" to these high-energy states [42] and find it to be of the order of 80% of the incident energy. Thus in order to reproduce the energy available for creating low-energy excitations in experiment, theoretically we require a significantly higher absorbed fluence to compensate for the energy "locked into" these high-energy states. In Co the empty d-band width is much larger than Ni and hence this effect is much more pronounced leading to the higher absorbed energy.

In this work, we have examined the origin of the shift downward in energy of the XAS L_3 edge peak in Ni, and the absence of a corresponding shift in the MCD L_3 edge peak. Using first-principles simulations of ultrafast demagnetization we are able to reproduce this effect and, moreover, predict that a strikingly different behavior will be found in Co with for this material the MCD peak shifting significantly upward in energy with only negligible change in the XAS peak position.

While in the past diverse explanations have been put forward for the peak shift in Ni, our work establishes a purely electronic origin for this effect. In Ni the nearly full d band restricts the energies above E_F into which charge can be excited, resulting in a charge excitation skewed to negative energies and a shift downward of the XAS peak. In Co, in contrast, the less full d band results in more evenly distributed excitation of charge from below to above E_F suppressing the peak shift. Spin-orbit-induced transitions from majority to minority channels below E_F result in a very small change in moment below E_F, with the demagnetization driven by a gain in negative moment (i.e., minority charge) above E_F. In Ni this is restricted to be close to E_F, yielding no MCD peak shift,

whereas in Co this extends to up to 2 eV above E_F resulting in a significant shift of the MCD peak.

We close this Letter by summarizing our three key predictions: (i) The XAS L_3 edge peak shift found in Ni will be much suppressed in Co, with instead a pronounced shift in the dichroic L_3 edge signal; (ii) as these peak shifts are driven by laser-induced changes in band occupation, they will occur for ultrafast pulses below the timescale of other excitations (e.g., magnons); and (iii) the magnitude of the shift will be dependent upon the laser pump pulse parameters with the XAS shift approximately proportional to the change in normalized moment, with a more complex dependence for the MCD peak shift in Co. Fully energy- and time-dependent experiments will be able to confirm the predictions made in the present work.

S. Sharma, J.K.D., C.v.k.S., and S.E. would like to thank the Deutsche Forschungsgemeinschaft for funding through Project ID 328545488 TRR227 (Projects No. A04 and No. A02). S. Shallcross would like to thank DFG for funding through Grant No. SH498/4-1. The authors acknowledge the North-German Supercomputing Alliance (HLRN) for providing HPC resources that have contributed to the research results reported in this Letter.

[1] J. Y. Bigot, M. Vomir, and E. Beaurepaire, Nat. Phys. **5**, 515 (2009).
[2] A. Kirilyuk, A. V. Kimel, and T. Rasing, Rev. Mod. Phys. **82**, 2731 (2010).
[3] M. Battiato, K. Carva, and P. M. Oppeneer, Phys. Rev. Lett. **105**, 027203 (2010).
[4] I. Radu, K. Vahaplar, C. Stamm, T. Kachel, N. Pontius, H. A. Dürr, T. A. Ostler, J. Barker, R. F. L. Evans, R. W. Chantrell, A. Tsukamoto, A. Itoh, A. Kirilyuk, T. Rasing, and A. V. Kimel, Nature (London) **472**, 205 (2011).
[5] A. Eschenlohr, M. Battiato, P. Maldonado, N. Pontius, T. Kachel, K. Holldack, R. Mitzner, A. Fhlisch, P. M. Oppeneer, and C. Stamm, Nat. Mater. **12**, 332 (2013).
[6] U. Bovensiepen, Nat. Phys. **5**, 461 (2009).
[7] J. K. Dewhurst, P. Elliott, S. Shallcross, E. K. U. Gross, and S. Sharma, Nano Lett. **18**, 1842 (2018).
[8] C. Jin, E. Y. Ma, O. Karni, E. C. Regan, F. Wang, and T. F. Heinz, Nat. Nanotechnol. **13**, 994 (2018).
[9] A. V. Kimel, A. M. Kalashnikova, A. Pogrebna, and A. K. Zvezdin, Phys. Rep. **852**, 1 (2020).
[10] F. Siegrist, J. A. Gessner, M. Ossiander, C. Denker, Y. P. Chang, M. C. Schroder, A. Guggenmos, Y. Cui, J. Walowski, U. Martens, J. K. Dewhurst, U. Kleineberg, M. Münzenberg, S. Sharma, and M. Schultze, Nature (London) **571**, 240 (2019).
[11] M. Hofherr, S. Häuser, J. K. Dewhurst, P. Tengdin, S. Sakshath, H. T. Nembach, S. T. Weber, J. M. Shaw, T. J. Silva, H. C. Kapteyn, M. Cinchetti, B. Rethfeld, M. M. Murnane, D. Steil, B. Stadtmüller, S. Sharma, M. Aeschlimann, and S. Mathias, Sci. Adv. **6**, eaay8717 (2020).
[12] C. Stamm, T. Kachel, N. Pontius, R. Mitzner, T. Quast, K. Holldack, S. Khan, C. Lupulescu, E. F. Aziz, M. Wietstruk, H. A. Dürr, and W. Eberhardt, Nat. Mater. **6**, 740 (2007).
[13] C. Boeglin, E. Beaurepaire, V. Halté, V. López-Flores, C. Stamm, N. Pontius, H. A. Dürr, and J.-Y. Bigot, Nature (London) **465**, 458 (2010).
[14] B. T. Thole, P. Carra, F. Sette, and G. van der Laan, Phys. Rev. Lett. **68**, 1943 (1992).
[15] P. Carra, B. T. Thole, M. Altarelli, and X. Wang, Phys. Rev. Lett. **70**, 694 (1993).
[16] C. Stamm, N. Pontius, T. Kachel, M. Wietstruk, and H. A. Dürr, Phys. Rev. B **81**, 104425 (2010).
[17] N. Bergeard, V. López-Flores, V. Halté, M. Hehn, C. Stamm, N. Pontius, E. Beaurepaire, and C. Boeglin, Nat. Commun. **5**, 3466 (2014).
[18] D. J. Higley, A. H. Reid, Z. Chen, L. L. Guyader, O. Hellwig, A. A. Lutman, T. Liu, P. Shafer, T. Chase, G. L. Dakovski, A. Mitra, E. Yuan, J. Schlappa, H. A. Dürr, W. F. Schlotter, and J. Stöhr, Nat. Commun. **10**, 5289 (2019).
[19] M. Hennecke, I. Radu, R. Abrudan, T. Kachel, K. Holldack, R. Mitzner, A. Tsukamoto, and S. Eisebitt, Phys. Rev. Lett. **122**, 157202 (2019).
[20] M. Hennes, B. Rösner, V. Chardonnet, G. S. Chiuzbaian, R. Delaunay, F. Döring, V. A. Guzenko, M. Hehn, R. Jarrier, A. Kleibert, M. Lebugle, J. Lüning, G. Malinowski, A. Merhe, D. Naumenko, I. P. Nikolov, I. Lopez-Quintas, E. Pedersoli, T. Savchenko, B. Watts *et al.*, Appl. Sci. **11**, 325 (2020).
[21] C. T. Chen, Y. U. Idzerda, H.-J. Lin, N. V. Smith, G. Meigs, E. Chaban, G. H. Ho, E. Pellegrin, and F. Sette, Phys. Rev. Lett. **75**, 152 (1995).
[22] L. L. Guyader, D. J. Higley, M. Pancaldi, T. Liu, Z. Chen, T. Chase, P. W. Granitzka, G. Coslovich, A. A. Lutman, G. L. Dakovski, W. F. Schlotter, P. Shafer, E. Arenholz, O. Hellwig, M. L. M. Lalieu, B. Koopmans, A. H. Reid, S. Bonetti, J. Stöhr, and H. A. Dürr, Appl. Phys. Lett. **120**, 032401 (2022).
[23] F. Willems, C. von Korff Schmising, C. Strüber, D. Schick, D. W. Engel, J. K. Dewhurst, P. Elliott, S. Sharma, and S. Eisebitt, Nat. Commun. **11**, 871 (2020).
[24] B. Rösner, B. Vodungbo, V. Chardonnet, F. Döring, V. A. Guzenko, M. Hennes, A. Kleibert, M. Lebugle, J. Lüning, N. Mahne, A. Merhe, D. Naumenko, I. P. Nikolov, I. Lopez-Quintas, E. Pedersoli, P. R. Ribic, T. Savchenko, B. Watts, M. Zangrando, F. Capotondi *et al.*, Struct. Dyn. **7**, 054302 (2020).
[25] T. Kachel, N. Pontius, C. Stamm, M. Wietstruk, E. F. Aziz, H. A. Dürr, W. Eberhardt, and F. M. F. de Groot, Phys. Rev. B **80**, 092404 (2009).
[26] K. Carva, D. Legut, and P. M. Oppeneer, Europhys. Lett. **86**, 57002 (2009).
[27] J. K. Dewhurst, F. Willems, P. Elliott, Q. Z. Li, C. von Korff Schmising, C. Strüber, D. W. Engel, S. Eisebitt, and S. Sharma, Phys. Rev. Lett. **124**, 077203 (2020).
[28] J. K. Dewhurst, S. Shallcross, P. Elliott, S. Eisebitt, C. v. Korff Schmising, and S. Sharma, Phys. Rev. B **104**, 054438 (2021).
[29] S. Sharma, S. Shallcross, P. Elliott, S. Eisebitt, C. v. Korff Schmising, and J. K. Dewhurst, Appl. Phys. Lett. **120**, 062409 (2022).
[30] K. Krieger, J. K. Dewhurst, P. Elliott, S. Sharma, and E. K. U. Gross, J. Chem. Theory Comput. **11**, 4870 (2015).

[31] J. K. Dewhurst, K. Krieger, S. Sharma, and E. K. U. Gross, Comput. Phys. Commun. **209**, 92 (2016).
[32] E. Runge and E. K. U. Gross, Phys. Rev. Lett. **52**, 997 (1984).
[33] D. J. Singh, *Planewaves, Pseudopotentials, and the LAPW Method* (Kluwer Academic Publishers, Boston, 1994).
[34] J. K. Dewhurst, S. Sharma *et al.*, http://elk.sourceforge.net.
[35] S. Sharma, J. K. Dewhurst, and E. K. U. Gross, in *First Principles Approaches to Spectroscopic Properties of Complex Materials*, edited by C. Di Valentin, S. Botti, and M. Cococcioni (Springer, Berlin, 2014), pp. 235–257.
[36] S. Sharma, J. K. Dewhurst, A. Sanna, and E. K. U. Gross, Phys. Rev. Lett. **107**, 186401 (2011).
[37] L. Hedin, Phys. Rev. **139**, A796 (1965).
[38] H. Ebert, Rep. Prog. Phys. **59**, 1665 (1996).
[39] R. Wu, D. Wang, and A. Freeman, J. Magn. Magn. Mater. **132**, 103 (1994).
[40] P. Elliott, T. Mueller, J. K. Dewhurst, and E. K. U. Gross, Sci. Rep. **6**, 38911 (2016).
[41] T. P. H. Sidiropoulos, N. Di Palo, D. E. Rivas, S. Severino, M. Reduzzi, B. Nandy, B. Bauerhenne, S. Krylow, T. Vasileiadis, T. Danz, P. Elliott, S. Sharma, K. Dewhurst, C. Ropers, Y. Joly, M. E. Garcia, M. Wolf, R. Ernstorfer, and J. Biegert, Phys. Rev. X **11**, 041060 (2021).
[42] C. Pellegrini, S. Sharma, J. K. Dewhurst, and A. Sanna, Phys. Rev. B **105**, 134425 (2022).